

Investigation of Mechanical Properties of Biodegradable AZ31 Magnesium Alloys with Calcium Addition

Thamarai Selvan ASHOKAN*, Surya SWAMYNATHAN, Santhosh SELVARANGAN

Department of Mechanical Engineering, Saveetha Engineering College (Autonomous), Chennai-602105, Tamil Nadu, India

<http://doi.org/10.5755/j02.ms.38398>

Received 8 August 2024; accepted 14 October 2024

In this research, the mechanical properties of as cast AZ31 magnesium alloys were investigated after adding 0.3 and 0.6 wt.% of calcium. As cast ingots of AZ31 Mg alloys with 0.3 and 0.6 wt.% of calcium were prepared under Argon environment. The specimens were made according to ASTM standards to perform tensile, compressive, and hardness tests. The microstructure and surface morphology of the alloys were analyzed using the images obtained from the optical microscope and scanning electron microscope (SEM) + EDAX. The yield strength (YS), ultimate tensile strength (UTS), ultimate compressive strength (UCS), percentage elongation, and Brinell hardness (HB) of these biodegradable Mg alloys were found. The addition of calcium to as cast AZ31+x wt.% Ca magnesium alloys (x = 0, 0.3 and 0.6) imparts good grain refinement and improves the mechanical properties with the formation of β -Mg₁₇Al₁₂ and Mg₂Ca intermediate metallic phases. The addition of calcium highly resists the formation of oxides and increases the strength of the alloy with fewer casting defects. The experimental results show that the yield strength increases up to 3.5 times with the increase of Ca content in AZ31 Mg alloys. The UTS is found up to 24 % with Brinell hardness showing an increase up to 53.3 %. The elongation increases from 10.5 % to 18 % with the addition of 0.3 wt.% of Ca but decrease to 12 % at 0.6 wt.% Ca. The mechanical properties and microstructure analysis of AZ31 + x wt.% Ca alloys prove their compatibility for making orthopedic implants in human bone surgery.

Keywords: AZ31 magnesium alloys, mechanical properties, grain refinement, biodegradable materials.

1. INTRODUCTION

In orthopedic surgery, magnesium alloys play a vital role in the past two decades as it does not require a second surgery to remove the implants after the bone gets cured [1]. This is due to the biodegradation behavior of the magnesium alloys that are used for making the implants whose biodegradation rate is almost equal to the curing rate of human bone. Mg in its pure form has very low strength (YS-20 MPa) and poor corrosive resistance. But its strength and corrosion resistance are improved by alloying with aluminium (Al), zinc (Zn), manganese (Mn), rare earth metals (REM), strontium (Sr), zirconium (Zr) and titanium (Ti) etc., [2–9]. However, the in-vivo and in-vitro properties of these Mg alloys are to be ensured before it is used for making such implants. The first generation of biomaterials was considered based on the physical properties and limited toxicity to human bone whereas the second-generation materials were tested with its ability to interact in biological environments and their biodegradation behaviour [5]. The magnesium alloys are predominant with its lowest density and good biocompatibility. The alloys like AZ21, AZ31, AZ61, AZ91, ZE60, etc., have become more promising biomaterials in recent decades. Binary alloys like Mg-Sn [4] and Mg-Sr [5] show positive results on cytotoxicity and biocompatibility tests performed. The Zr in the tertiary alloys Mg-Zr-Sr [6] and Mg-Zn-Zr [7] impart good mechanical properties by grain refinement and increasing ductility. However, the huge difference in mechanical and material properties of these alloys when compared to human

bone would result in unwanted stresses induced into the injured bone [8] affecting the bone growth.

The yield strength of a human cortical bone ranges from 90 MPa – 140 MPa [1, 5, 7], and the ultimate compressive strength is 164–240 MPa. The ductility varies between 1.0–2.1 % and its density nearer to the density of AZ31 (1.73 gcm⁻³) attracts the researchers towards Mg alloys in AZ series. In the AZ series, the main alloying elements are Al, Zn and Mn with more than 90 % concentration of magnesium. Al and Zn impart good mechanical strength and corrosive resistance, but their percentage weight compositions play a vital role in determining these properties [9]. Aluminium content of more than 6 wt.% in composition in Mg alloy leads to more corrosiveness and poor biocompatibility in cytotoxicity and cell culture tests, which endangers the applications of Mg alloys in orthopedic surgery [10].

The addition of Ti in AZ31 also performs greater grain refinement and produces very high tensile strengths at extrusion [11]. The biocompatibility of Ti is also quite good [12] so it will find its contribution in biodegradable implants. The addition of Calcium (Ca) in Mg alloys shows greater grain refinement, increase in mechanical properties and improved corrosion resistance with good biocompatibility [13–15]. It also resists the oxidation of Mg and Ca in the alloys; moreover, Ca is an important constituent in human bone. The ignition and oxidation of Mg are greatly controlled by the addition of Ca and CaO [14]. The biodegradation behaviour of Mg-Ca alloys [9, 16, 17] found its application in orthopedic surgery and

* Corresponding author: A. Thamarai Selvan
E-mail: thamaraiselvan@saveetha.ac.in

proved its biodegradation after inserting on a rabbit bone. But the addition of Ca more than 2.0 wt.% in pure Mg weakens the grain boundaries thus reduction in mechanical properties which is observed in Mg-Ca alloys [12]. Mg-0.2Zn-0.1Ca is used to produce highly ductile biodegradable soft clips for orthopedic applications [3].

An investigation of Ce, Sr, and Ca in AZ31 alloy shows a faster rate in the formation of intermetallic phases with Ce whereas Sr and Ca refine the grain structure of the alloy [18]. An improved mechanical property of AZ91 alloy is obtained with 0.5–2.0 wt.% of Ca but the increased Ca content reduces the $Mg_{17}Al_{12}$ phases with the formation of weak Mg_2Ca [19, 20]. The formation of oxides helps the alloys in initiating their degradation at the same time, a high concentration of oxides will reduce the strength of the alloys. The YS and UTS can be increased by reducing impurities in AZ31 alloy [21]. Though calcium is an important constituent of human bone, the optimum quantity of Ca to use has to be determined to improve the performance of these AZ31 biodegradable materials.

In this research, ascast AZ31 alloys with 0.0, 0.3, and 0.6 wt.% of Ca were fabricated and tested to find the influence of Ca in microstructures, grain refinement and mechanical properties and its compatibility to make it suitable for biodegradable orthopedic implants such as screws and nuts.

2. MATERIALS AND METHODS

2.1. Fabrication of Mg alloys

The ingots of ascast AZ31 magnesium alloys in addition with 0.3 and 0.6 wt.% of Ca are prepared in an electric resistance crucible furnace of 10 Kg capacity. AZ31 alloys are prepared by melting magnesium ingots between 690 °C to 720 °C in a controlled environment under $SF_6 + CO_2$. A flux is also added to prevent oxidation of the magnesium before charging. The alloying elements of aluminium (Al–3 %), zinc (Zn–1 %) and manganese (Mn–0.02 %) were added to the magnesium in the preheated crucible at 400 °C. The mixture is steered for 15 minutes so that all the alloying elements melt and diffuse into the molten magnesium. Then it is stirred for 10 minutes to have a uniform dispersion of Al, Zn and Mn with Mg. The molten mixture was cast into rectangular ingots of size 300 mm × 100 mm × 30 mm on a preheated die mould. The AZ31 alloys with 0.0, 0.3 and 0.6 wt.% of calcium were prepared where Ca is added around 680 °C. The calcium initially is ignited and oxidized in the molten alloy since calcium floats on the melt and hence a cover flux added to prevent ignition and to have uniform dispersion of the calcium in the melt. The compositions of the alloying elements of AZ31 Mg alloys fabricated are shown in Table 1.

2.2. Microstructure analysis

An optical microscope (OM) is used to observe the microstructure of the grains (Fig. 2) and a scanning electron microscope (SEM) with energy-dispersive spectroscopy (EDS) is used to analyze the surface morphology (Fig. 3) for the presence of intermediate metallic phases. The phase compositions (Fig. 4) are identified by energy-dispersive

spectroscopy (EDS). The composition of all elements and intermetallic phases in all AZ31 Mg alloys are quantified with the EDX analysis.

Table 1. Chemical compositions of magnesium alloys AZ31 added with calcium

Mg alloys	Al	Zn	Mn	Ca	Mg
AZ31	2.76	0.89	<0.02	0	Rest
AZ31 + 0.3 Ca	2.57	0.92	<0.02	<0.3	Rest
AZ31 + 0.6 Ca	2.91	0.95	<0.02	<0.6	Rest

The specimens were prepared and polished in polish grinders with 100 to 400 grid emery belts. Initially, the belt of higher grid number is used for rough polish and lower grid numbered belts till mirrorlike surface finish is obtained. Then the specimen surface is etched with a solution consisting of acetic acid (2 ml), picric acid (6 g), water (1 ml), phosphoric acid (0.5 ml), and ethanol (100 ml) to observe the microstructures and grain boundaries clearly.

2.3. Tensile and compression tests

The tensile specimens were prepared according to ASTM E8/E8M and E9 standards for finding the yield strength (YS), ultimate tensile strength (UTS), and % elongation of the alloys made. The specimens (Fig. 1) were made into cylindrical shapes of ϕ 12.5 mm × 50 mm gauge length with 25 mm threaded heads on either side machined to the required dimensions.

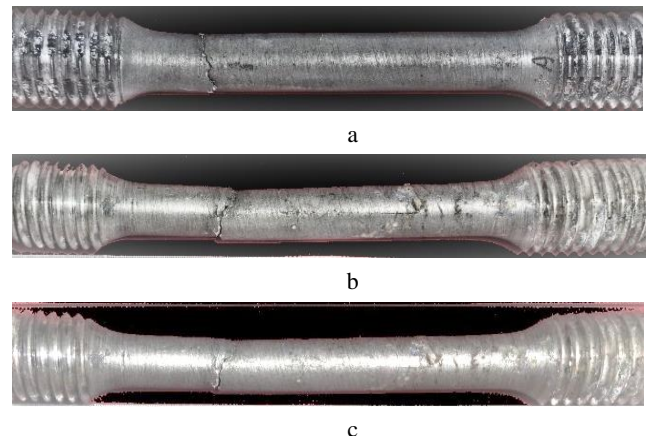


Fig. 1. Sample specimens after tensile testing: a–AZ31 alloy; b–AZ31 + 0.3 Ca alloy; c–AZ31 + 0.6Ca alloy

The tensile tests were carried out in universal testing machine INSTRON5984 with 150 KN. An extensometer is fitted in the setup to measure strain. The experimental tests were conducted at room temperature. The specimens for compression tests were prepared with the dimensions: ϕ 11 mm diameter and 16.5 mm length.

2.4. Hardness

The Brinell hardness (HB) of AZ31 magnesium alloys and with 0.0, 0.3, and 0.6 wt.% of Ca was found using Brinell hardness testing machine. Each sample was tested at five different locations on the specimen surface. The specimens for finding the hardness were prepared by machining into cylindrical shapes for the required dimensions. The hardness values in HB are shown in Table 2.

3. RESULTS

3.1. Microstructure, XRD and SEM+EDAX analysis

The Fig. 2 shows the microstructures of AZ31 and AZ31 + x Ca alloys. In Fig. 2, the micrograph of AZ31 alloy shows the grain structure of the alloy and widespread intermetallic $Mg_{17}Al_{12}$ phases. These $Mg_{17}Al_{12}$ phases (Fig. 3) are uniformly dispersed on the grain boundaries of AZ31 Mg alloy which are very important for the strength of alloys [1, 3]. The shape of these phases is mostly dendrite and few take oval and rod shaped precipitates. The grain size of AZ31 alloy is measured as per ASTM E112 [7] and it ranges between 206 – 266 μm .

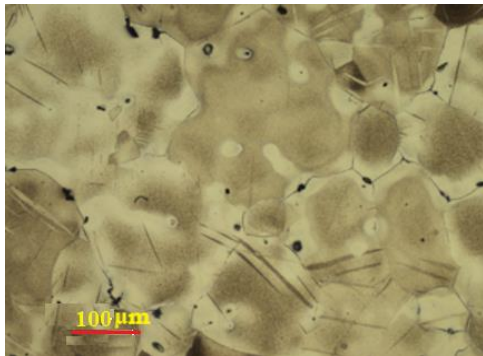


Fig. 2. Microstructure of AZ31 Mg alloy

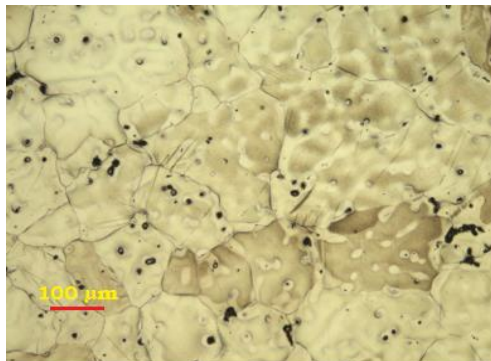


Fig. 3. Microstructure of AZ31 + 0.3 Ca Mg alloy

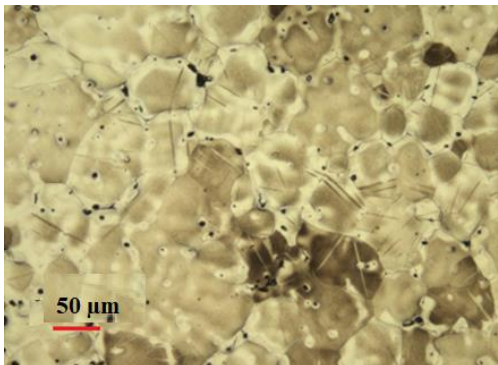


Fig. 4. Microstructure of AZ31 + 0.6 Ca Mg alloy

The distribution of secondary phases of $Mg_{17}Al_{12}$ on the grain boundary of AZ31 Mg alloy (Fig. 2). The Fig. 3 shows the micrographs of AZ31 + 0.3 Ca alloy and intermetallic phases present on the grain boundaries. The grain size of AZ31 + 0.3 Ca alloy ranges from 170 μm – 190 μm . From the Fig. 4, the grain boundaries are more visible due to the

improved grain refinement with an oncrease in Ca content in AZ31 with 0.6 wt.% Ca. The calcium improves the grain refinement, but decreases the size of the dendrite shaped $Mg_{17}Al_{12}$ phases. And it reduces its grain size to 58 – 85 μm .

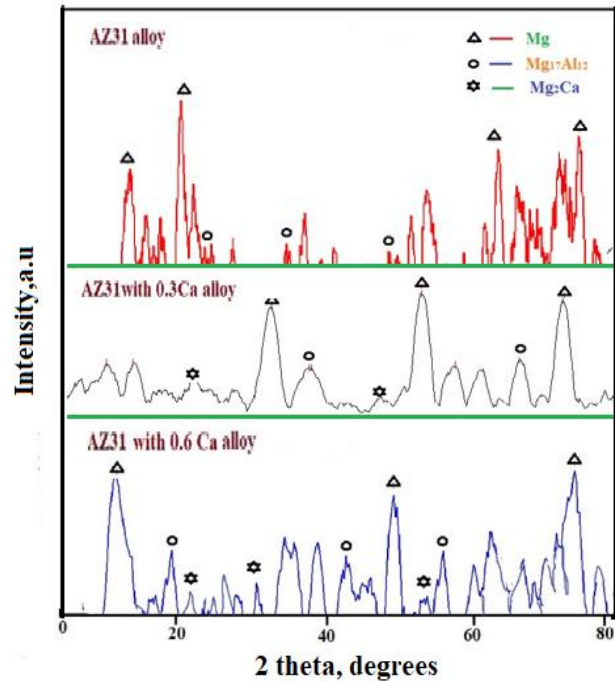


Fig. 5. XRD patterns of AZ31 alloys

The X-ray Diffraction (XRD) patterns of AZ31 + x Ca alloys are show in Fig. 5. The results revealed that the sample has 97.9, 84.3 and 98.7 % of amorphous structure in AZ31, AZ31 + 0.3 Ca, and AZ31 + 0.6 Ca alloys respectively. Since the samples are less crystalline, the graphs are not smooth. The XRD of AZ31 alloy at angles 18.309°, and 64.625°, with intensities 13.1479, and 5.73825 counts reveals the presence of α -Mg phase and the phases of $Mg_{17}Al_{12}$ are shown in the graph. For AZ31+ 0.3Ca, the intensities 101.711 and 100.487, 57.4025 and 39.4761, 20.4417 and 21.8669 counts and for AZ31 + 0.6 Ca alloys, the intensities 34.8047, 19.3642 and 7.36545 reveal the presence of α -Mg phase, $Mg_{17}Al_{12}$ and Mg_2Ca phases respectively.

The SEM image shows the surface morphology of AZ31 Mg alloys (Fig. 4 a–c). From the results of EDX analysis, the intermediate phases $Mg_{17}Al_{12}$ and Mg_2Ca formed in the AZ31 + x Ca alloys are shown. The intermediate Mg_2Ca phases formed in AZ31 + 0.6 Ca alloy shown (Fig. 4 c) are oval in shape and distributed in large amount than with that of AZ31 + 0.3 Ca alloy due to an increase in Ca content. The size of Mg_2Ca phases is small compared to that of $Mg_{17}Al_{12}$. The presence of Mg_2Ca phases in AZ31 + x Ca alloys exhibits good biocompatibility and produces promising results on degradation under in-vivo experiments which is much needed for biodegradation [17].

3.2. Mechanical properties of AZ31 alloys

Five specimens of each AZ31 Mg alloys with 0.0, 0.3, 0.6 wt.% of Ca were made as per the ASTM standards to find the mechanical properties of yield strength (YS), ultimate tensile strength (UTS), ultimate compressive

strength (UCS), Percentage elongation and Brinell hardness. The observed values of these mechanical properties are given in Table 2.

Table 2. Mechanical properties of AZ31 Mg alloys with calcium addition

Mg alloys	YS	UTS	UCS	%e	Hardness, HB
	MPa				
AZ31	61±4	174±6	286±3	10.0–10.5	43.7–45.1
AZ31+0.3 Ca	76±5	215±4	315±5	16.5–18.0	44.0–45.9
AZ31+0.6 Ca	150±8	206±5	293±4	11.5–12.5	68.2–71.0

3.3. Mechanical properties

Tensile and compression tests were carried out as per ASTM E8-04 and ASTM E9-09 standards respectively [7]. The tensile properties shown in the Table 2 are measured from 5 specimens prepared from as cast AZ31, AZ31 + 0.3 Ca and AZ31 + 0.6 Ca alloys. The yield strength at 0.2 % increases with an increase in Ca addition from 0.0 to 0.6 wt.% and but UTS shows an increase only up to 0.3 wt.% of Ca. Similar effects are also observed in UCS and percentage elongation of the alloys. The measures of UTS, UCS and percentage elongation decrease for the alloys after 0.3 wt.% of Ca addition. These properties get decreased at 0.6 wt.% of Ca addition.

Generally, the hardness of the metal alloys is measured in Brinell hardness (HB). The average values of the result were taken as the mean hardness of the alloys. The measured hardness was found with only fewer deviations in its values at each location and hence we can understand that the hardness of the alloys is uniform throughout the sample substrates. The hardness values for the alloys are shown in Table 2.

4. DISCUSSION

From Fig. 2–Fig. 4, the micrographs of as cast AZ31 alloy observed with an optical microscope (OM) show the grain boundaries and SEM images (Fig. 6 a–c) show intermediate metallic phases of $Mg_{17}Al_{12}$ formed at the grain boundaries of AZ31 Mg alloy.

The presence of these $Mg_{17}Al_{12}$ phases imparts good strength to AZ31 Mg alloys [1–3]. The dendrite shape microstructures of intermetallic phases in AZ31 alloy is a good sign for the proper mixing of various elements in the alloy [16, 18]. Some pores also exist nearer to the grain boundaries or almost on the boundary itself which may endanger the elastic properties of the ascast AZ31 alloy, but these pores also act as initiators for the biodegradation of the material [1, 8]. However, the existence of minimum quantity of these voids shows that the strength of the alloys could not be affected to a greater amount.

From the investigation made on the microstructure of AZ31 + 0.3 Ca (Fig. 3) and AZ31 + 0.6 Ca (Fig. 4), it is observed that the grain structures are highly refined with the increase in the addition of calcium. The larger grain structure of AZ31 alloy (Fig. 2) is reduced (Fig. 3) after the addition of 0.3 wt.% of Ca and Fig. 4 shows improved further grain refinement in the microstructure of AZ31 + 0.6 Ca alloy. This ensures that grain refinement is highly improved in AZ31 Mg alloy with the increase in Ca content [14, 18]. The grain refinement is also observed in

AZ91 Mg alloys [1, 19] with Ca addition but new intermediate phases of Al_2Ca are also formed along with $Mg_{17}Al_{12}$.

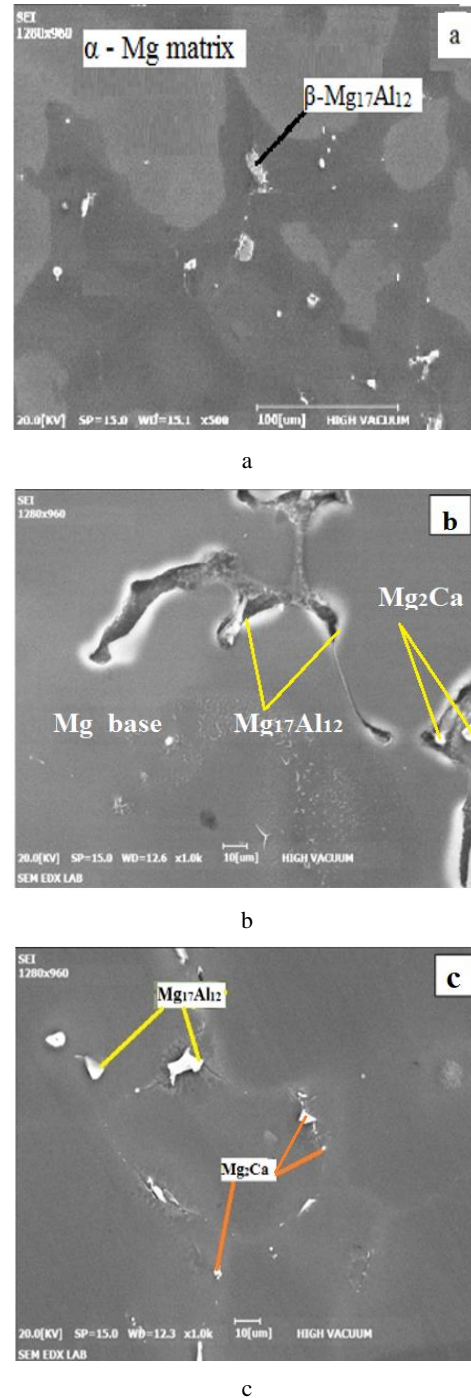


Fig. 6. SEM images: a–secondary phases of AZ31 alloy; b–secondary phases of AZ31 + 0.3 Ca alloy; c–secondary phases of AZ31 + 0.6 Ca alloy

These Al_2Ca phases affect the grain growth and refinement restricting the deformation of grain structures. The Al_2Ca phase formation depends on the Al content which should be greater than 4 wt.% [20]. In AZ31 alloy, the content of Al is less than 3 wt.% and hence there is no possibility for the formation of Al_2Ca phases and hence larger grain refinement is achieved. From the Fig. 2–Fig. 4, it is found that the addition of Ca in AZ31 Mg alloy decreases the quantity of the $Mg_{17}Al_{12}$ phase [20] present in

the microstructures. The grain size and $Mg_{17}Al_{12}$ phases on the grain boundaries decrease with an increase in Ca content. The reason for the reduction in $Mg_{17}Al_{12}$ phases is the lower solubility of Al in Mg with an increase in Ca content. Only less amount of Mg_2Ca phase formations (Fig. 6 b) is observed in AZ31 + 0.3 Ca Mg alloy as its formation is purely dependent on calcium content [13]. From the Fig. 6 c, AZ31 + 0.6 Ca alloy contains large amount of Mg_2Ca phases inside the grain boundaries. The images obtained from a scanning electron microscope also reveal the presence of intermediate metallic $Mg_{17}Al_{12}$ and Mg_2Ca phases in alloys containing calcium.

In Fig. 6 a–c, two different regions (dark and bright) are observed due to difference in wt.% of Mg and compositions of the alloying elements. The EDAX analysis at two locations (Fig. 7 a) of AZ31 alloy shows the presence of oxides of the alloying elements that also enhances the degradation behaviour of these biodegradable materials [16].

However, the presence of a large amount of oxide films reduces the strength of the Mg alloys [9]. In Fig. 7 b, it is observed only a small quantity of oxides present in AZ31 + 0.3 Ca alloy. But there is no evidence for the formation of oxides (Fig. 7 c) in case of AZ31 with 0.6 wt. % of Ca. This proves that with the addition of Ca, formation of metal oxides in AZ31 alloy could be highly avoided with increase in the content. In AZ31 + 0.6 Ca alloy, there is no trace of oxide formation, and thus calcium content of more than 0.5 wt.% in AZ31 alloys reduces the formation of oxides. This resistance to oxide formations is another reason for reduction in UTS, UCS and elongation as the alloy becomes more ductile with earlier brittleness at fracture. This type of fracture is often referred as quasi-cleavage fracture where materials will have dimple brittleness before rupture.

According to the Hall-Petch relationship, fine grains result in increased yield strength. The addition of Ca in AZ31 Mg alloys enhances grain refinement of microstructures to larger extent [21]. The yield strength at 0.2 % increases with increase in Ca content in order of $AZ31 < AZ31 + 0.3 \text{ Ca} < AZ31 + 0.6 \text{ Ca}$ (Fig. 8). There is a drastic increase in yield strength between 0.3–0.6 wt.% of Ca addition. The Ca addition up to 0.3 wt.% improves the UTS of AZ31 + x Ca alloys where UTS increases from 21.176 KN to 26.524 KN. However, with 0.6 wt.% of Ca, UTS slightly gets reduced to 24.68 KN. More than 0.5 wt.% of Ca addition results in reduction of UTS [13, 14]. The increase in Ca content imparts higher rate of strain hardening in the alloys and becomes more plastic before rupture [21]. The brittleness is imparted after plastic deformation causing premature failure when the Ca is more than 0.3 wt.%.

When 1.5 wt.% of Ca is added to AZ31 alloy [12], more amount of Al_2Ca is formed which affects the grain growth. But no such formation of Al_2Ca phases in AZ31 + 0.3 Ca and AZ31 + 0.6 Ca alloys as more than 1 mass unit of Al requires 1.35 mass unit of Ca [13] to form Al_2Ca precipitates or phases. Due to grain refinement with the addition of Ca, $Mg_{17}Al_{12}$ phases get reduced in quantity in AZ31 alloys and hence the UTS increases (Fig. 8) in order of $AZ31 < AZ31 + 0.6 \text{ Ca} < AZ31 + 0.3 \text{ Ca}$. In case of Compressive strength, AZ31 alloy with 0, 0.3, 0.6 wt.% of

Ca additions yields an average of 286, 315 and 293 MPa respectively. The result shows that addition of Ca also influences the compressive strength of the alloys. The compressive strength of AZ31 Mg alloys with Ca addition behaves same as that of UTS of the alloys.

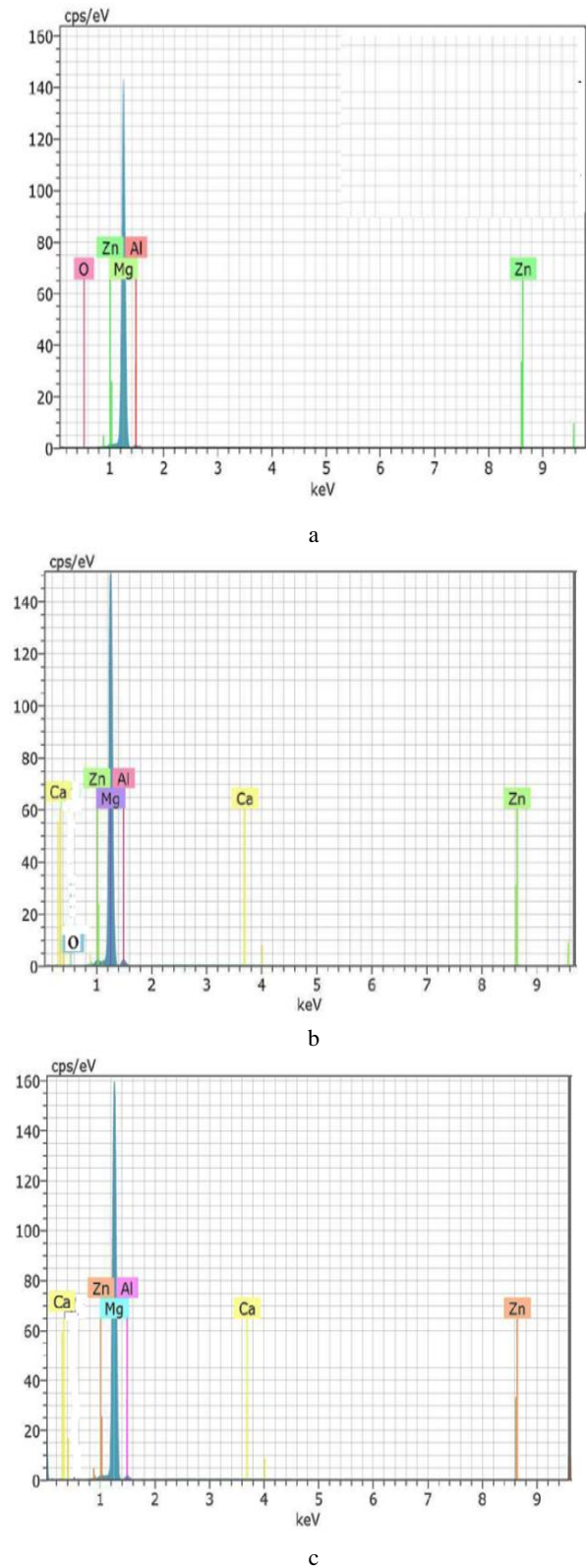


Fig. 7. EDX graph: a–AZ31 Mg alloy; b–AZ31+0.3Ca Mg alloy; c – AZ31+0.6Ca Mg

The melting point of $Mg_{17}Al_{12}$ phase is around 1079 °C and that of Al_2Ca is 763 °C [2] and hence the stability of solid $Mg_{17}Al_{12}$ phase dispersed in AZ31 Mg alloys imparts good yield strength, UTS, % elongation and hardness than pure Mg and some other Mg alloys [14, 15].

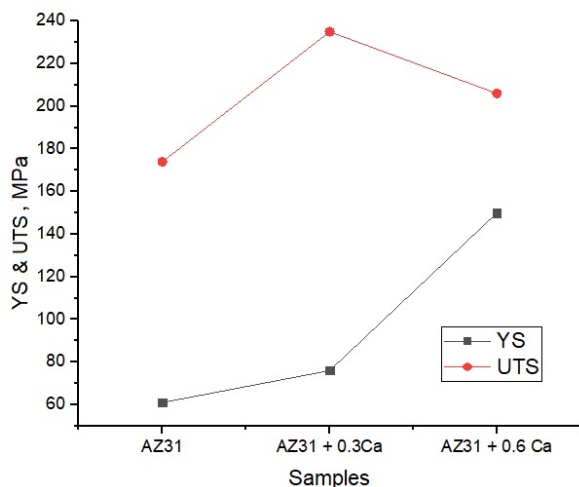


Fig. 8. Yield strengths and ultimate tensile strengths of AZ31 + x Ca alloys

Another reason for these irregular variations in UTS, elongations and UCS is the local strain caused by the interstitial elements at lattices surrounding the dislocations which increase the stresses to remove the dislocations and unlock grain boundaries [21]. Due to the local straining, the material after yield reaches a plastic stage and the free energy variations occur according to the plasticity at each stage leading to cleavage fracture and hence irregular variations of UTS, UCS and elongations are observed in the AZ31 magnesium alloys with Ca addition i.e., those properties get decreased from 0.3 to 0.6 wt.%. But in general view, the ductility of AZ31 alloys is greatly improved with the addition of calcium.

From Table 2, it is understood that there is no much variations in Brinell hardness of AZ31 and AZ31 + 0.3 Ca alloys but there a steep increase in the hardness of AZ31 + 0.6 Ca alloy. Adding more than 0.3 wt.% of Ca in AZ31 Mg alloys results in drastic increase in its hardness. This is due to highly improved grain refinement observed in the microstructure and formation of secondary phases [22] with increase in Ca content. Also, with increase in the quantity Mg_2Ca phases, high hardness is imparted in these Mg alloys with Ca addition.

In as cast biodegradable Mg-1.0Sr alloy [5], the tensile yield strength, UTS and UCS are found as 56, 92.67 and 243.6 MPa respectively which are dominated by as cast AZ31 Mg alloys. Another biodegradable Mg-Zr-Sr alloy has lowered tensile and compressive properties [6] compared to proposed AZ31 Mg alloys. Generally, the yield strength of a cortical human bone ranges between 90–140 MPa [10] and excess yield strength imparts unwanted stress shield [8] in materials that is used for biodegradable implants of orthopedic surgery. The grain size is also highly reduced to 11.2–15.6 μm which can lead to poor degradation rate [1, 10, 12]. The tensile properties and hardness of materials greater than that of human bone would cause undesirable stress induced into the bone on

which implants are fixed. It causes stress shielding during of human bone surgery [8]. The yield and compression strengths are very important as far as in biodegradable implants with UTS as less important.

The typical human bone has 5–25 % of elongation [1, 6]. In this research, as cast AZ31 Mg alloys with Ca addition proves its in-vitro compatibility with their YS, UTS, UCS and its hardness values proves its suitability and importance, thus AZ31 + x Ca alloys can be used for making biodegradable implants which dominates most of the as cast and extruded magnesium alloys in in-vitro properties.

5. CONCLUSIONS

The microstructure of the AZ31 alloys with Ca addition shows improved grain refinement with the increase in Ca content. The grain size drastically gets reduced from an average of 230 μm (AZ31 alloy) to 75 μm (AZ31 + 0.6 Ca alloy) which is a notable sign for improvement of mechanical properties of the alloys.

The secondary intermediate metallic phases $Mg_{17}Al_{12}$ and Mg_2Ca formed in AZ31+xCa alloys improves the mechanical properties like YS, UTS, UCS, % elongation and hardness (HB) so that AZ31+xCa alloys are more suitable to make biodegradable implants in orthopedic surgery. However more that 0.3–0.6 wt.% of Ca content slightly reduces UTS, UCS, % elongation properties due to increase in quantity of Mg_2Ca and decrease in size and quantity of $Mg_{17}Al_{12}$ phases. But YS and hardness are highly improved with increase in Ca addition by restricting the formation of oxides in the alloys in greater extent.

The presence of pores in microstructures of as cast AZ31 Mg alloys with and without Ca addition initiates the degradation behaviour of the alloys. The mechanical properties of the alloys are highly influenced by the formation of intermetallic phases, grain refinement and restricted oxide formations. Thus, the results on microstructure and mechanical properties of AZ31 + x Ca alloys prove its compatibility for making biodegradable implants.

REFERENCES

1. Mythili, P., Janis, L., Kristine, S.A., Dagnija, L., Alain, L., Liga, B.C. Biodegradable Materials and Metallic Implants *Journal of Functional Biomaterials* 8 (44) 2017: pp. 44. <https://doi.org/10.3390/jfb8040044>
2. Meisam, S., Yuebin, G. Biodegradable Orthopedic Magnesium-Calcium (MgCa) Alloys, Processing, and Corrosion Performance *Materials* 5(1) 2012: pp. 135–155. <https://doi.org/10.3390/ma5010135>
3. Ikeo, N., Nakamura, R., Naka, K., Hashimoto, T., Yoshida, T., Urade, T., Fukushima, K., Yabuuchi, H., Fukumoto, T., Ku, Y., Mukai, T. Fabrication of a Magnesium Alloy with Excellent Ductility for Biodegradable Clips *Acta Biomaterialia* 29 2015: pp. 468–475. <https://doi.org/10.1016/j.actbio.2015.10.023>
4. Chaoyong, Z., Fusheng, P., Shuang, Z., Hucheng, P., Kai, S., Aitao, T. Microstructure, Corrosion Behavior and Cytotoxicity of Biodegradable Mg–Sn Implant Alloys

Prepared by Sub-rapid Solidification *Materials Science and Engineering C* 54 2015: pp. 245–251.
<https://doi.org/10.1016/j.msec.2015.05.042>

5. **Yuxiang, W., Di, T., Renguo, G., Ning, W., Yingqiu, S., Tong, C., Junqiao, L.** Microstructures, Mechanical Properties, and Degradation Behaviors of Heat-Treated Mg-Sr Alloys as Potential Biodegradable Implant Materials *Journal of the Mechanical Behavior of Biomedical Materials* 77 2017: pp. 47–57.
<http://doi.org/10.1016/j.jmbbm.2017.08.028>.
6. **Yuncang, Li., Cuie, W., Dolly, M., Ragamouni, S., Nemani, H., Gopal, P., Peter, H.** Mg–Zr–Sr Alloys as Biodegradable Implant Materials *Acta Biomaterialia* 8 2012: pp. 3177–3188.
<http://doi.org/10.1016/j.actbio.2012.04.028>
7. **Daeho, H., Partha, S., Da-Tren, C., Boeun, L., Boyce, E.C., Zongqing, T., Zhongyun, D., Prashant, N.K.** In vitro Degradation and Cytotoxicity Response of Mg–4% Zn–0.5% Zr (ZK40) Alloy as a Potential Biodegradable Material *Acta Biomaterialia* 9 (10) 2013: pp. 8534–8547.
<https://doi.org/10.1016/j.actbio.2013.07.001>
8. **Pilliar, R.M., Cameron, H.U., Binnington, A.G., Szivek, J., Macnab, I.** Bone Ingrowth and Stress Shielding with a Porous Surface Coated Fracture Fixation Plate *Journal of Biomedical Materials Research* 13 (5) 1979: pp. 799–810.
<https://doi.org/10.1002/jbm.820130510>
9. **Annett, K., Nina von der, H., Dirk, B., Christian, K., Friedrich, W.B., Henning, W., Andrea, M.L.** Degradation Behaviour and Mechanical Properties of Magnesium Implants in Rabbit Tibiae *Journal of Materials Science* 45 2010: pp. 624–632.
<https://doi.org/10.1007/s10853-009-3936-3>
10. **Lida, H., Zhen, L., Yu, P., Li, D., Xinlin, L., Yufeng, Z., Li, L.** In Vitro and In Vivo Studies on Biodegradable Magnesium Alloy *Progress in Natural Science: Materials International* 24 (5) 2014: pp. 466–471.
<https://doi.org/10.1016/j.pnsc.2014.09.002>
11. **Adnan, I.O., Raghad, Hememat, S.** Investigation on the Effect of Titanium (Ti) Addition to the Mg-AZ31 Alloy in the As cast and After Extrusion Conditions on its Metallurgical and Mechanical Characteristics *Materials Science and Engineering* 146 (1) 2014: pp. 12–26.
<https://doi.org/10.1088/1757-899X/146/1/012026>
12. **Long, L., Ming, Z., Ye, L., Jie, Z., Ling, Q., Yuxiao, L.** Corrosion and Biocompatibility Improvement of Magnesium-Based Alloys as Bone Implant Materials: A Review *Regenerative Biomaterials* 4 (2) 2017: pp. 129–137.
<https://doi.org/10.1093/rb/rbx004>
13. **Seong-Ho, H.A., Jin-Kyu, L., Hyung-Ho, J., Seung-Boo, J., Kim-Shae, K.** Behavior of CaO and Calcium in Pure Magnesium *Rare Metals* 25 (6) 2006: pp. 150–154.
[https://doi.org/10.1016/S1001-0521\(08\)60071-6](https://doi.org/10.1016/S1001-0521(08)60071-6)
14. **Naoto, S., Kunio, F., Masafumi, N., Hisashi, M.** Effect of Ca Addition on the High-Temperature Deformation Behavior of AZ31 Magnesium Alloy *The Minerals, Metals and Materials Society* 2013: pp. 1203–1209.
https://doi.org/10.1007/978-3-319-48764-9_148
15. **Hamid Reza, B.R., Idris, M.H., Mohammed Rafiq, A.K., Saeed, F.** Microstructure Analysis and Corrosion Behavior of Biodegradable Mg–Ca, Implant Alloys *Materials and Design* 33 2012: pp. 88–97.
<https://doi.org/10.1016/j.matdes.2011.06.057>
16. **Feser, K., Kietzmann, M., Ba Umer, W., Krause, F.W.** Effects of Degradable Mg–Ca Alloys on Dendritic Cell Function *Journal of Biomaterials Applications* 25 (7) 2011: pp. 685–697.
<https://doi.org/10.1177/0885328209360424>
17. **Mukhametkaliyev, T., Surmeneva, M., Surmenev, R., Mathan, B.K.** Hydroxyapatite Coating on Biodegradable AZ31 and Mg-Ca Alloys Prepared by RF Magnetron Sputtering *American Institute of Physics* 1688 (1) 2015: pp. 1–4
<https://doi.org/10.1063/1.4936001>
18. **Shang, L., Junga, I.H., Yue, S., Verma, R., Essadiqi, E.** An Investigation of Formation of Second Phases in Micro Alloyed, AZ31 Mg Alloys with Ca, Sr and Ce *Journal of Alloys and Compounds* 492 (1–2) 2010: pp. 173–183.
<https://doi.org/10.1016/j.jallcom.2009.11.159>
19. **Wang, Q., Chen, W., Zeng, X., Lu, Y., Ding, W., Zhu, Y., Xu, X.** Effects of Ca Addition on the Microstructure and Mechanical Properties of AZ91 Magnesium Alloy *Journal of Materials Science* 36 (12) 2001: pp. 3035–3040.
<https://doi.org/10.1023/A:1017927109291>
20. **Redeemina, C.B., Yu, F., Hai, H.** Microstructure and Mechanical Properties of AZ91 Magnesium Alloy with Minor Additions of Sm, Si and Ca Elements *Research & Development* 16 (5) 2019: pp. 319–325.
<https://doi.org/10.1007/s41230-019-9067-9>
21. **Chen, X., Fusheng, P., Jianjun, M., Zengshu, Z.** Improved Mechanical Properties in AZ31 Magnesium Alloys Induced by Impurity Reduction *Journal of Wuhan University of Technology-Mater. Sci. Ed.* 28 (6) 2013: pp. 1207–1211.
<https://doi.org/10.1007/s11595-013-0846-7>
22. **Kara, I.H., Yusef, T.A.I., Ahlatci, H., Türen, Y.** Effect of Ca and Ce on Wear Behavior of Hot-Rolled AZ31 Mg Alloys *Acta Physica Polonica A* 137 2020: pp. 557–560.
<https://doi.org/https://doi.org/10.12693/APhysPolA.137.557>



© Ashokan et al. 2025 Open Access This article is distributed under the terms of the Creative Commons Attribution 4.0 International License (<http://creativecommons.org/licenses/by/4.0/>), which permits unrestricted use, distribution, and reproduction in any medium, provided you give appropriate credit to the original author(s) and the source, provide a link to the Creative Commons license, and indicate if changes were made.